Egypt. J. Chem. **Vol. 66**, No. 10 pp. 389 - 401 (2023)

Egyptian Journal of Chemistry

http://ejchem.journals.ekb.eg/

Metal Complexes of 1,4-Bis(2-Hydroxyethyl) Piperazine: Thermodynamic and Theoretical Approach

Mohamed R. Shehata*[1], Mohamed M. Shoukry[1] and Mahmoud A. Mabrouk[2]

[1]*Department of Chemistry, Faculty of Science, Cairo University, Giza,12613, Egypt*

[2]*Egyptian Academy for Engineering & Advanced Technology (EAE & AT) Affiliated to Ministry of Military Production, Cairo, Egypt*

Abstract

In the present study, the acid-base equilibria of 1,4-bis(2-hydroxyethyl)piperazine (BHEB) and the formation equilibria of complexes with the metal ions Cu(II), Ni(II), Co(II),and Zn(II) are investigated using the potentiometric technique. The acid-dissociation constants of BHEP in the protonated form and the formation constants of the complexes are determined using the Miniquad-75 program in the temperature range (of15oC - 35oC). The thermodynamic parameters were determined and discussed. The concentration distribution diagrams of the complexes are evaluated. The effect of metal ion properties such as atomic number, ionic radius, electronegativity, and ionization potential are investigated. The complexes were synthesized and characterized by elemental analysis and mass spectra. Density Functional Theory (DFT) calculations have been performed to study the equilibrium geometry of 1,4-bis(2-hydroxyethyl)piperazine and its complexes. The optimization of the structure of the complexes reveals that CuIIand CoIIcomplexes have distorted octahedral geometry. NiIIcomplex has a distorted square planar geometry.ZnIIcomplex has a distorted tetrahedral geometry. The calculated total energies, energies of the highest occupied molecular orbital (HOMO), energies of the lowest unoccupied molecular orbital (LUMO), and dipole moments are reported. The N---N distance for uncoordinated 1,4-bis(2-hydroxyethyl)piperazine is calculated to be 2.870 Å and decreased to 2.588 Å, 2.491 Å, 2.502 Å, 2.479 Å, and 2.552 Å for Cu(II), Co(II), Ni(II) and Zn(II) complexes respectively. Also, bonds connected to N atoms are elongated upon complex formation. The interactions with the receptors as breast cancer oxidoreductase were feasible as evidencedby Docking analysis.

Keywords: 1,4-bis(2-hydroxyethyl)piperazine, metal complexes, speciation study, DFT calculation, docking.

1. Introduction

The piperazine moiety has significant activities. Piperazine derivatives have useful diverse pharmacological activities. [1-5] They have antianginal [6,7] antidepressant [8,9], antipsychotic[10,11], antidiabetic [4], antihistaminic5, and hypolipidemic [6] activities. Some piperazine derivatives are used as flavoring agents6. Now drug companies produce piperazine derivatives through various research development processes and will become available commercially for therapeutic uses. Shortly piperazine drugs will have a role in various disease treatments and will replace the existing organic-based pharmaceuticals.

The behavior of piperazine derivatives and their interaction with metal ions existing in biological fluids did not receive significant attention. The investigation of complex formation equilibria of piperazines with metal ions commonly existing in biological fluids is supporting the biological

*Corresponding author e-mail: mrshehata@sci.cu.edu.eg;(Mohamed R. Shehata).
EJCHEM use only: Received date 18 January 2023; revised date 25 February 2023; accepted date 12 March 2023
DOI: 10.21608/EJCHEM.2023.187495.7476

significance of this class of compounds. In continuation of our previous work on metal complexes of biological significance including those with piperazine compounds[12-17] the present investigation deals with the interaction of some selected metal ions with 1,4-bis(2-hydroxyethyl)piperazine. The complex formation equilibria are investigated. The solid complexes were synthesized, and characterized and the antitumor activity was screened. The equilibrium geometry of homopiperazine and its complex was studied by Density Functional Theory (DFT) calculations. Molecular docking analysis has been carried out to investigate the interaction with the receptors of breast cancer oxidoreductase.

2. Experimental

2.1 Materials and reagents

The ligand 1,4-bis(2-hydroxyethyl)piperazine was purchased from Sigma Chem. Co. The metal salts used are $CuCl_2.2H_2O$, $CoCl_2.6H_2O$, $NiCl_2.6H_2O$, and $ZnCl_2.2H_2O$. They were obtained from Sigma Chem. Co. Metal salt solutions were prepared and standardized as reported previously[18]. NaOH solution (titrant) was prepared and standardized against potassium hydrogen phthalate solution. The ligand solution was prepared in the diportonated form in HCl solution. All solutions were prepared in deionized water.

2.2. Synthesis of metal complexes

1.0 mmoleof $CuCl_2.2H_2O$, $CoCl_2.6H_2O$, $NiCl_2.6H_2O$, or $ZnCl_2.2H_2O$ was dissolved in 10 ml of water and mixed with 1.0 mmole portions of 1,4-bis(2-hydroxyethyl)-piperazine. The mixture was stirred and refluxed at 70 ºC for 4 hours. The complexes were precipitated on cooling. The precipitated complexes were filtered off and washed with water, ethanol and diethyl ether. The yield was from 80 to 90%. Anal. Calcd. data for the complexes are:

$Cu(BHEP)Cl_2(H_2O)_2$: blue color, $CuC_8H_{22}Cl_2N_2O_4$ (MW = 344.72): C, 27.87; H,6.43; N, 8.13 Found: C, 27.69; H, 6.48; N, 8.09%.

$Co(BHEP)Cl_2(H_2O)_2$: pink color $CoC8H_{22}Cl_2N_2O_4$(MW = 340.11): C, 28.25; H, 6.52; N, 8.24; Found: C, 28.16; H, 6.61; N, 8.12%.

$Ni(BHEP)Cl_2$: green color $NiC_8H_{18}Cl_2N_2O_2$(MW = 303.84): C, 31.62; H, 5.97; N, 9.22; Found: C, 31.57; H, 6.02; N, 9.10%.

$Zn(BHEP)Cl_2$: white color$ZnC_8H_{18}Cl_2N_2O_2$(MW = 310.52): C, 30.94; H, 5.84; N, 9.02; Found: C, 30.81; H, 5.91; N, 8.97%.

2.3. Procedure and Measuring Techniques

The solid complex compositions were evidenced by elemental analysis; carbon, hydrogen, and nitrogen were carried out on a Perkin-Elmer 240C elemental analyzer. The mass spectrum was recorded by EI ionization mode using MS-5988 GS-MS Hewlett-Packard instrument at 70 eV.

Potentiometric measurements were used to determine the acid-dissociation of the ligand and formation constants of the metal complexes in 0.1M $NaNO_3$ solution at the temperature of 15, 20, 25, 30 and 35°C. The titrations were carried out in a computer-controlled Metrohm 751 Titrino. The temperature of the titration cell was maintained by circulating water from a thermostat water bath. Standard buffer solutions [19]as potassium hydrogen phthalate, (pH= 4.008) and a mixture of KH_2PO_4 and Na_2HPO_4 (pH=6.865) were used to calibrate the titroprocessor and electrode.

The acid dissociation constants of the ligand were determined by titrating 40 ml of the diprotonatedligand solution (1.25×10^{-3}M). The formation constants of the complexes were determined by titrating 40 ml of the solution containing metal ions (1.25×10^{-3}M) and Ligand (2.5×10^{-3} M). All potentiometric titrations were carried out at 25°± 0.05°C, in a double-walled glass cell of 50 ml capacity. The temperature of all solutions was adjusted by the circulation of thermostated water through the outer jacket of the cell. The solutions were stirred with a magnetic stirrer, and all titrations were performed in triplicate at an ionic strength of 0.1M (KCl).

All titrations were performed in a purified nitrogen atmosphere, using aqueous 0.05 M NaOH as titrant. The pH meter readings were converted into hydrogen ion concentration by titrating HCl solution ($0.05\ mol \cdot dm^{-3}$) with NaOH solution ($0.05\ mol \cdot dm^{-3}$) at 25°C and I = $0.1\ mol \cdot dm^{-3}$ $NaNO_3$. The pH is plotted against p[H]. The relationship pH−p[H] = 0.05 was observed. [OH^-] value was calculated using a pK_w value of 13.90. For the variable temperature studies the following values of pK_w were employed [20,21] at 15°C (pK_w = 14.25) at 20°C (pK_w = 14.07), at 25°C (pK_w = 13.90), 30°C (pK_w = 13.74) and 35°C (pK_w = 13.69)

The equilibrium constant of the protonation of BHEP and the formation constant of its metal complexes was evaluated from titration data. The equilibrium was defined by Eq. 1.

$$lM + pL + rH \rightleftharpoons M_lL_pH_r \quad (1)$$

Where M, L and H represent metal ion and ligand and proton; respectively.

The formation constants were evaluated using the computer program MINIQUAD-75 [22]. The stoichiometry and stability constants of the complexes formed were determined by trying various possible composition models. The model selected was that which gave the best statistical fit and was chemically consistent with the magnitude of various residuals, as described elsewhere [22]. The fitted model was tested by comparing the experimental titration data points and the theoretical curve calculated from the values of the acid dissociation constant of the ligand and formation constants of the corresponding complexes.Tables 1 and 2, list the equilibrium constants together with their standard deviation derived from the MINIQUAD output. The Concentration distribution diagram was obtained using the program SPECIES [23].

2.4. Molecular modeling studies

Density Functional Theory (DFT) calculations have been executed to study the equilibrium geometry of the ligand and complexes at the B3LYP level of theory, where C, H, N, O and Cl atoms with basis set 6-311G++(dp) and metal atoms with basis set LANL2DZ, respectively using Gaussian 09 program[24].

2.5 Molecular docking

The molecular docking investigations were done using MOA2019 software [25]. The binding modes of the most active site of the receptor of breast cancer oxidoreductase (PDB ID: 3HB5) [26] were estimated. The optimized structure of BHEP and complexes from the output of Gaussian09 calculations were created in PDB file format. The crystal structures of the receptors were downloaded from the protein data bank (http://www.rcsb.org/pdb).

3. Results and discussion

3.1. Characterization of the complex

The solid complexes were synthesized and characterized by elemental analysis. The analytical data revealed the formation of the complexes of 1:1 stoichiometry. The composition of the complexes was further evidenced by the mass spectra. The molecular ion peaks of the Cu(II),Co(II), Ni(II) and Zn(II) complexes were detected at m/z = 345, 340, 336, 303and 311, respectively Figure 1.Single crystal of Pd(BHEP)Cl_2 was obtained previously and shows the coordination of Pd to the two N atoms and two Cl in square planar structure leaving the two OH uncoordinated [13].

The potentiometric titration curves of protonated BHEP in the presence and absence of metal ions are compared. The metal ion-BHEP curves are lower than that of BHEP, Figure 2. This corresponds to the formation of the complex through the release of hydrogen ions

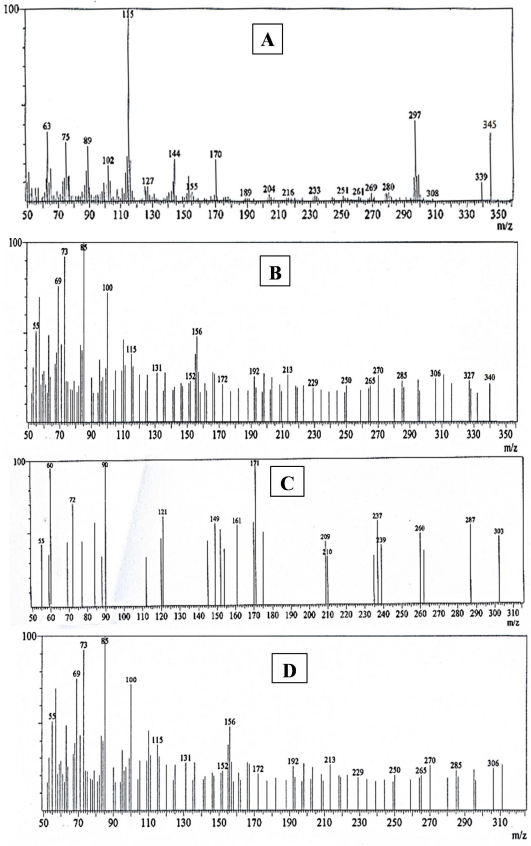

Fig. 1: The Mass spectra of the Cu (A), Co (B), Ni (C), and Zn (D) complexes

3.2. Acid-Base equilibria of 1,4-bis(2-hydroxyethyl)piperazine

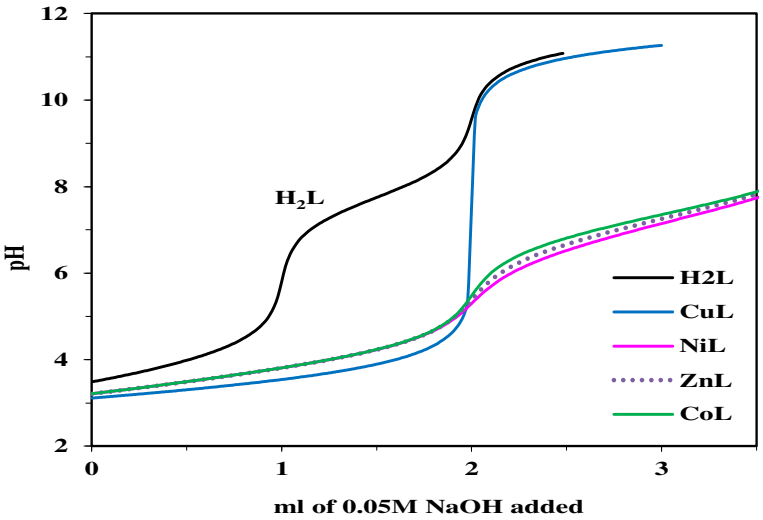

Fig. 2: Potentiometric titration curves of protonated BHEP (H_2L^{2+}) and its metal complexes at 25ºC

The potentiometric titration curve of 1,4-bis(2-hydroxyethyl)-piperazine in the protonated form (H_2L^{2+}) shows two buffer regions, in Figure 2. The first one is corresponding to the neutralization of the first more acidic protonated imino group (pK_{a1} = 3.70 at 25°C), yielding HL^+ species. The next buffer region corresponds to the deprotonation of the second protonated imino group, giving the species L (pK_{a2} = 7.65 at 25°C). The concentration distribution of the protonated forms of BHEP is given in Figure 3. The diprotonated form predominates at low pH up to pH = 3.8. The mono-protonated species prevails between a pH of 3.8 to 7.8, with a maximum concentration of ~98% at a pH of 5.6. The neutral form of BHEP prevails above the pH of 7.8.

3.3. Complex formation equilibria of 1,4-bis(2-hydroxyethyl)piperazine

The potentiometric data are fitted assuming the formation of metal complexes of stoichiometric ratios 1:1 and 1:2 (metal: BHEP). The validity of the complex formation model was tested by comparing the potentiometric titration data with the theoretically simulated curve obtained from the protonation constants of BHEP and the formation constants of the corresponding complex species. The complex-forming abilities of the transition metal ions are frequently characterized by stability orders. The value of logK1 arranged in the order Co< Ni< Cu > Zn is by Irving-Williams order [27,28] for divalent metals of 3d series. The ligand field will give Cu^{2+} some extra stabilization due to the tetragonal distortion of the octahedral symmetry [29-31]. Estimation of equilibrium concentrations (speciation) of metal (II) complexes as a function of pH provides a useful picture of metal ion binding in solutions.

Table 1
Stepwise stability constants for the complexation of (BHEP) with divalent metal ions in aqueous solution at 0.1 mole dm^{-3} $NaNO_3$ at 25 ºC

M L H[a]	**logβ[b]**		
	H_2L	Cu-L	
0 1 1	7.64(0.02)	-	
0 1 2	11.35(0.03)	-	
1 1 0	-	7.72(0.02)	
1 2 0	-	14.01(0.04)	
	Ni-L	Co-L	Zn-L
1 1 0	3.66(0.02)	3.45(0.03)	3.18(0.02)
1 2 0	5.98(0.04)	5.36(0.04)	5.02(0.03)

[a]M, L and H are the stoichiometric coefficients corresponding to divalent metal ions, BHEP and H^+, respectively; [b]Standard deviations are given in parentheses

The concentration distribution diagrams are given in Figure 3. The concentrations of metal-ligand complexes increase with increasing pH. In the species distribution pattern for Cu(BHEP) complex, taken as a representative of metal-ligand complexes, the 1:1 complex starts to form at pH 2 and predominates at pH 3.8 with a maximum formation percentage of 72%. The 1:2 complex starts to form at pH 3 and its concentration increases with the increase in pH. From the biological point of view, both 1:1 and 1:2 complexes are existing in the biological pH range.

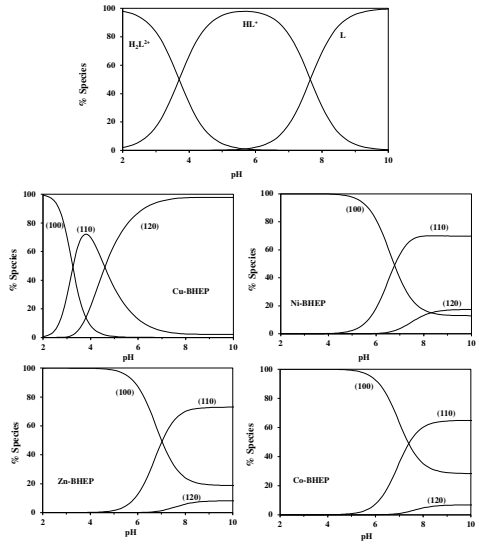

Fig. 3: Concentration distribution diagrams of protonated BHEP and its metal complexes

3.4. Effect of temperature

The thermodynamic parameters ΔH° and ΔS° were obtained by linear least-squares fit of lnK vs. 1/T with an intercept of ΔS°/R and a slope of –ΔH°/R according to the following equation[31].

$$\Delta G^\circ = \Delta H^\circ - T\Delta S^\circ$$

$$\Delta G^\circ = -RT \ln K$$

$$\ln K = -\Delta H^\circ/RT + \Delta S^\circ/R$$

3.4.1 Effect of temperature on protonation of BHEP

Dissociation constants of protonated BHEP, H_2L^{2+} at different temperatures and 0.1M ionic strength are given in Table 2.

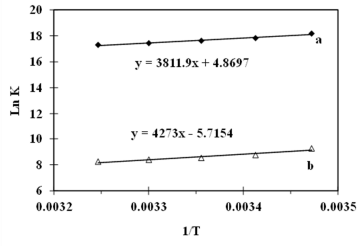

Fig. 4. Effect of temperature on the protonation of BHEP, where a and b correspond to equations 1 and 2 in Table 3, respectively

Table 2
Dissociation constants of BHEP in water at different temperatures at 0.1M ionic strength

L H[a]			log β[b]
	15 °C	**20 °C**	**25 °C**
1 1	7.89(0.01)	7.74(0.01)	7.65(0.01)
1 2	11.91(0.02)	11.54(0.02)	11.35(0.02)
pKa1	7.89	7.74	7.65
pKa2	4.02	3.80	3.70
	30 °C	35 °C	
1 1	7.57(0.01)	7.51(0.01)	
1 2	11.21(0.02)	11.09(0.02)	
pKa1	7.57	7.51	
pKa2	3.64	3.58	

[a]L and H are the stoichiometric coefficients corresponding to BHEP and H^+, respectively; [b]Standard deviations are given in parentheses

The thermodynamic parameters ΔH°, ΔS° and ΔG° are summarized in Table 4 and interpreted as follows: The protonated reactions of BHEP (1) and (2), indicated in Table 4, are exothermic. Three factors[32-35] affect protonation reactions: **(i)** the interaction of hydrogen ions with BHEP is an exothermic process, **(ii)**the desolvation of BHEP which is endothermic **(iii)**

the configuration and the rearrangement of the hydrogen bonds around the free and protonated BHEP. The positive ΔS° in equation (1) indicates that BHEP (L) is highly solvated by water molecules (more order) than the protonated ligand, HL^+.

3.4.2 Effect of temperature on the stability constant of Metals- BHEP complexes

The stability constants of Metals-BHEP complexes at different temperatures are given in Table 3 and Figure 4. Figures 5 and 6 show the stepwise complex formation reactions ($M^{2+} + L \rightleftharpoons ML^{2+}$ and $ML^{2+} + L \rightleftharpoons ML_2^{2+}$, respectively).

The complexation reactions in Table 4 between metal ions and BHEP are exothermic. The stability constants of the complexes formed at different temperatures were calculated and included in Table 4.

Table 3
Stepwise Formation constants of Metal-BHEP complexes in water at different temperatures and 0.1M ionic strength

Metal	logK		
M2+ + L ⇌ ML2+			
	15 °C	20 °C	25 °C
Co2+	3.39(0.05)	3.28(0.03)	3.18(0.02)
Zn2+	3.68(0.06)	3.56(0.04)	3.45(0.03)
Ni2+	3.89(0.03)	3.78(0.05)	3.66(0.02)
Cu2+	8.13(0.03)	7.91(0.01)	7.72(0.02)
	30 °C	35 °C	
Co2+	3.07(0.02)	2.95(0.01)	
Zn2+	3.36(0.03)	3.25(0.02)	
Ni2+	3.53(0.03)	3.42(0.01)	
Cu2+	7.61(0.02)	7.45(0.01)	
ML2+ + L ⇌ ML22+			
	15 °C	20 °C	25 °C
Co2+	2.08(0.05)	1.96(0.03)	1.84(0.02)
Zn2+	2.21(0.06)	2.11(0.04)	1.91(0.03)
Ni2+	2.57(0.03)	2.45(0.05)	2.32(0.02)
Cu2+	6.58(0.01)	6.42(0.01)	6.29(0.04)
	30 °C	35 °C	
Co2+	1.72(0.02)	1.60(0.01)	
Zn2+	1.81(0.03)	1.71(0.02)	
Ni2+	2.21(0.03)	2.11(0.01)	
Cu2+	6.15(0.03)	5.99(0.01)	

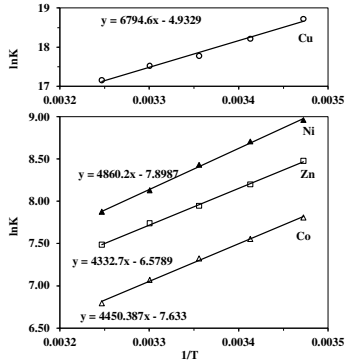

Fig. 5. Effect of temperature on Metals-BHEP system ($M^{2+} + L \rightleftharpoons ML^{2+}$)

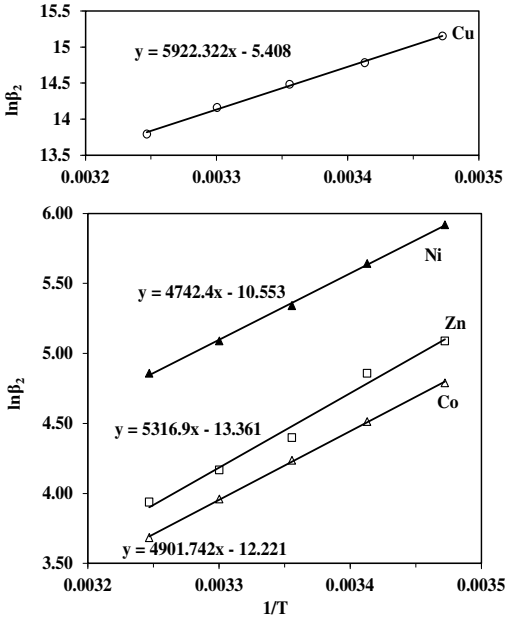

Fig. 6. Effect of temperature on Metals-BHEP system ($M^+ + 2L \rightleftharpoons ML_2^{2+}$)

These values decrease with increasing temperature, confirming that the complexation process is more favorable at lower temperatures The thermodynamic parameters of metal complexes were calculated by a procedure like that used for the dissociation of BHEP and are recorded in Table 4. It is known that the divalent metal ions exist in solution as octahedrally hydrated species[36] and the obtained values of ΔH° and ΔS° can then be considered as the sum of two contributions: (a) release of H_2O molecules and (b) metal-ligand bond formation.

From these results the following conclusions can be made:

1. All values of ΔG° for complexation are negative, indicating the spontaneity of the chelation process.
2. The negative values of ΔH°, show that the chelation process is exothermic, indicating that the complexation reactions are favoredat low temperatures.
3. The high negative enthalpy change contributes to the favorable free energy change of the complex formation reactions.

Table 4
Thermodynamic parameters for the stepwise stability constants of protonated BHEP and Metals-BHEP complexes.[a]

Metal	ΔH° kJmol^{-1}	ΔS° JK^{-1}mol^{-1}	ΔG° kJmol^{-1}
1)L + H^+ ⇌ LH^+			
	-31.7(0.5)	40.5(0.6)	-43.8(0.6)
2)LH^+ + H^+ ⇌ LH_2^{2+}			
	-35.5(0.5)	-47.5(0.7)	-21.4(0.3)
3)M^{2+} + L ⇌ ML^{2+}			
Co^{2+}	-37.0(0.5)	-63.5(0.9)	-18.1(0.2)
Zn^{2+}	-36.0(0.5)	-54.7(0.8)	-19.7(0.3)
Ni^{2+}	-40.4(0.6)	-65.7(0.9)	-20.8(0.3)
Cu^{2+}	-56.5(0.8)	-41.1(0.6)	-44.3(0.7)
4)M^{2+} + 2L ⇌ ML_2^{2+}			
Co^{2+}	-40.7(0.6)	-101.6(1.1)	-10.5(0.2)
Zn^{2+}	-44.2(0.7)	-111.1(1.2)	-11.1(0.2)
Ni^{2+}	-39.4(0.6)	-87.7(0.9)	-13.3(0.3)
Cu^{2+}	-49.2(0.7)	-44.9(0.2)	-35.8(0.5)

[a]where L is unprotonated BHEP; standard deviations are given in parentheses

3.5. Molecular DFT Calculation

3.5.1 Molecular DFT Calculation of Ligand BHEP

Figure 7 shows the optimized structures of the ligand BHEP as the lowest energy configurations. The natural charges obtained from Natural Bond Orbital Analysis (NBO) show that the more negative active sites are in order O1 (-0.731) > O2 (-0.730) > N2 (-0.576) > N1 (-0.571). The metal ions prefer bidentate coordination to N1 and N2 forming a 5-membered ring.

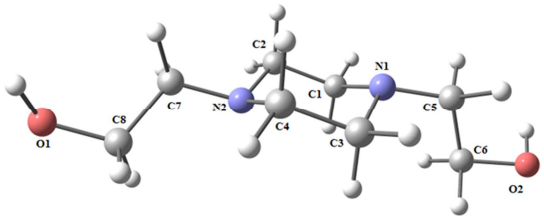

Fig. 7. Effect of temperature on Metals-BHEP

3.5.2 Molecular DFT Calculation of Copper and Cobalt Complexes

The optimized structures of Cu(BHEP)$(H_2O)_2Cl_2$, andCo(BHEP)$(H_2O)_2Cl_2$ complexes as the lowest energy configurations are shown in Figure 8. respectively, which indicates that these atoms are almost in one plane. The bite angles (N1-Cu-N2 = 72.53° and N1-Co-N2 = 74.42°) are lower than 90° due to chelation. The bond angles in the octahedral geometry of Cu- and Co-complexes are ranging from 72.53° to 104.3°, from 74.42° to 99.28°, and 71.06° to 96.90°, respectively, Table 5.

The distance between donor atoms N1----N2 involved in coordination is decreased upon complex formation from 2.860Å (in free ligand) to 2.588Å, 2.488Å and 2.500Å in Cu- and Co-complexes, respectively. The copper and cobalt atoms are six-coordinate in a distorted-octahedral geometry with O3 and O4 of water molecules in the axial position. The dihedral angles of atoms N1, N2, *Cl*1 and *Cl*2 in Cu-, and Co-complexes are -7.196°, -0.795° and -1.316°; The natural charges computed from the NBO analysis on the coordinated atoms are (Cu (+0.683), N1 (-0.524), N2 (-0.524), O3 (-0.913), O4 (-0.913), *Cl*1(-0.625) and *Cl*2(-0.625) in Cu-complex) and (Co (+0.483), N1 (-0.490), N2 (-0.490), O3 (-0.898), O4 (-0.898), *Cl*1(-0.587) and *Cl*2(-0.587) in Co-complex).

Table 5
Important optimized bond lengths (Å) and bond angles (°) of Cu(BHEP)$(H_2O)_2Cl_2$, Co(BHEP)$(H_2O)_2Cl_2$, Ni(BHEP)Cl_2 and Zn(BHEP)Cl_2 complexes

Cu(II) complex	**Co(II) complex**
Cu-N1=2.132	Co-N1=2.057
Cu-N2=2.132	Co-N2=2.057
Cu-*Cl*1=2.416	Co-*Cl*1=2.392
Cu-*Cl*2=2.416	Co-*Cl*2=2.392
Cu-O3=2.473	Co-O3=2.324
Cu-O4=2.473	Co-O4=2.324
N1-Cu-N2=72.53	N1-Co-N2=74.42
N1-Cu-*Cl*2=96.07	N1-Co-*Cl*2=96.18
N2-Cu-*Cl*1=96.07	N2-Co-*Cl*1=96.18
*Cl*1-Cu-*Cl*2=95.71	*Cl*1-Co-*Cl*2=93.23
O3-Cu-N1=104.3	O3-Co-N1=97.84
O3-Cu-N2=97.48	O3-Co-N2=99.28
O3-Cu-*Cl*1=81.84	O3-Co-*Cl*1=84.06
O3-Cu-*Cl*2=80.04	O3-Co-*Cl*2=81.19
O4-Cu-N1=97.48	O4-Co-N1=99.28
O4-Cu-N2=104.3	O4-Co-N2=97.84
O4-Cu-*Cl*1=80.04	O4-Co-*Cl*1=81.19
O4-Cu-*Cl*2=81.84	O4-Co-*Cl*2=84.06
N1-Cu-*Cl*1=167.5	N1-Co-*Cl*1=170.6
N2-Cu-*Cl*2=167.5	N2-Co-*Cl*2=170.6
O3-Cu-O4=152.9	O3-Co-O4=158.5
N1-N2-Cl1-Cl2=-7.196*	N1-N2-*Cl*1-*Cl*2=-0.795*
Ni(II) complex	**Zn(II) complex**
Ni-N1=2.016	Zn-N1=2.185
Ni-N2=2.016	Zn-N2=2.185
Ni–*Cl*1=2.246	Zn-*Cl*1=2.327
Ni–*Cl*2=2.246	Zn-*Cl*2=2.327
N1-Ni-N2=75.87	N1-Zn-N2=71.37
N1-Ni-*Cl*2=96.49	N1-Zn-*C*l1=109.9
N2-Ni-*Cl*1=96.49	N2-Zn-Cl2=109.9
Cl1-Ni-Cl2=93.96	Cl1-Zn-Cl2=128.6
N1-Ni-*Cl*1=164.4	
N2-Ni-*Cl*2=164.4	
N1-N2-*Cl*1-*Cl*2=-7.51*	

*dihedral angle

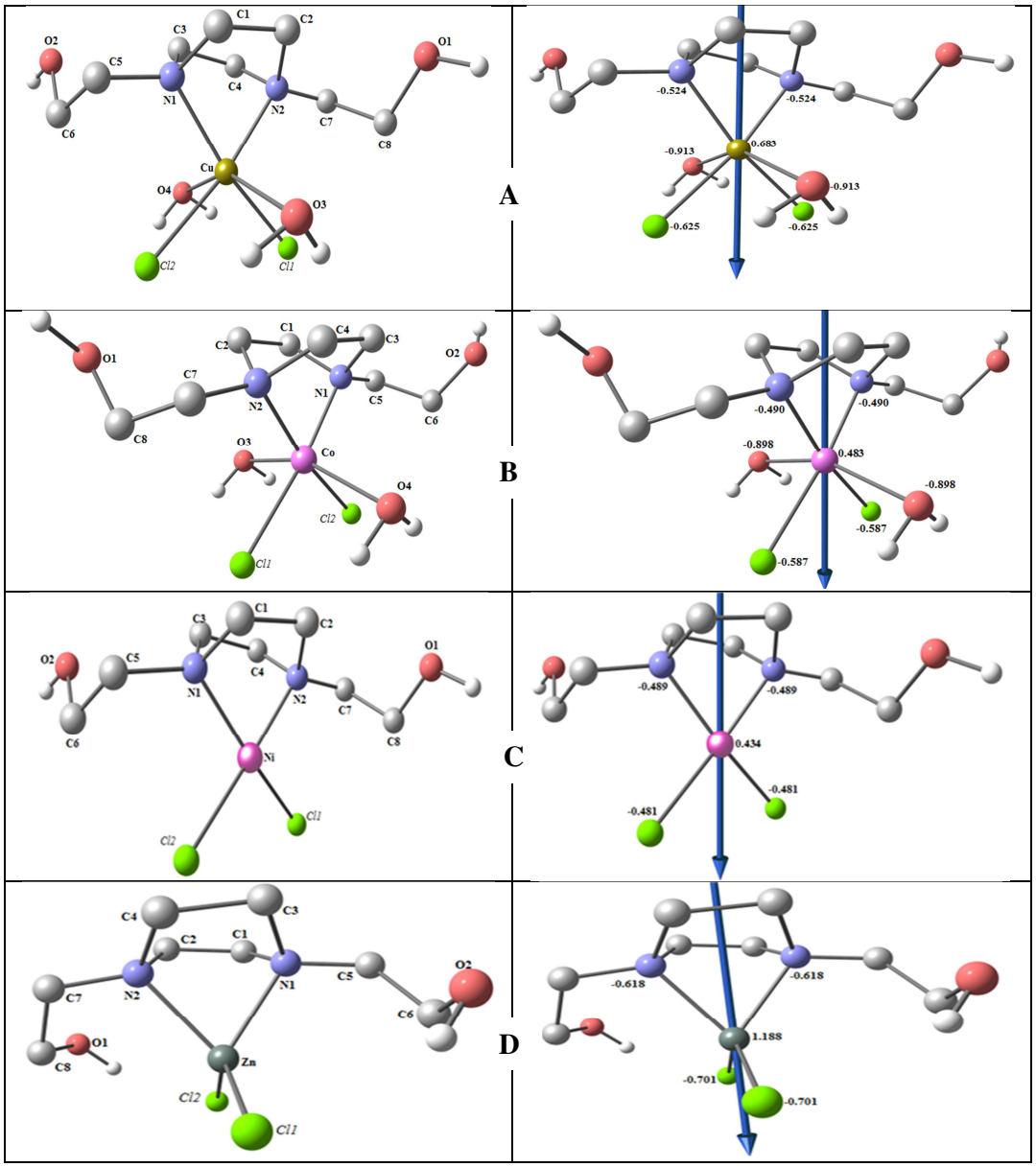

Fig. 8. The optimized structure, the vector of the dipole moment, and the natural charges on active centres of Cu(BHEP)$(H_2O)_2Cl_2$(**A**), Co(BHEP)$(H_2O)_2Cl_2$(**B**), Ni(BHEP)Cl_2(**C**) and Zn(BHEP)Cl_2(**D**) complexes

3.5.3 Molecular DFT Calculation of Nickel(II) and Zinc(II) complexes:

Ni(II) complex has a distorted square planar geometry as found from the optimization of its structure, Figure 8. The atoms N1, N2, *Cl*1 and *Cl*2 are coordinated to Ni(II) ion and exist in one plane deviated by -7.51° (dihedral angle). The bite angle N1-Ni-N2 (75.87°) is lower than 90° due to chelation. The bond angles in the square are ranging from 75.87° to 96.49°, Table 5. N1-N2-*Cl*1-*Cl*2=-7.51*

A distorted-tetrahedral geometry is deduced from the optimization of the Zn(II) complex structure, Figure 9. The Zn atom is tetracoordinate with a bit angle N1-Zn-N2 71.37°. This is lower than the expected bond angle for a regular tetrahedral structure (109°), due to

chelation. The other bond angles are close to 109 in the range of 71.9° to 110.4°, Table 5.

The distance between the coordinated donor atoms N1----N2 is decreased upon complex formation from 2.860Å (in free ligand) to 2.480Å and 2.549 Å in Ni- and Zn-complexes, respectively.

The natural charges computed from the NBO analysis on the coordinated atoms are (Ni (+0.434), N1 (-0.489), N2 (-0.489), *Cl*1(-0.481) and *Cl*2(-0.481) in Ni-complex and Zn (+1.188), N1 (-0.618), N2 (-0.618), *Cl*1 (-0.701), *Cl*2 (-0.701) in Zn-complex.

Table 6
Calculated energies of BHEB and the complexes at B3LYP/LANL2DZ

	E[a]	HOMO[b]	LUMO[c]	E_g[d]	Dipole moment[e]
BHEP	-575.77	-5.9596	-0.4210	5.5386	1.9066
Cu complex	-1845.16	-6.5828	-3.6415	2.9413	6.7514
Co complex	-1794.11	-6.2834	-2.1007	4.1827	9.3720
Ni complex	-1665.44	-6.2301	-2.4934	3.7367	9.5784
Zn complex	-1561.77	-7.4677	-0.5834	6.8843	7.6938

[a]E: the total energy (a.u.). [b]HOMO: highest occupied molecular orbital (eV). [c]LUMO: lowest unoccupied molecular orbital (eV). [d]E_g: the energy gab =E_{LUMO}- E_{HOMO} (eV). [e] dipole moment (Debye).

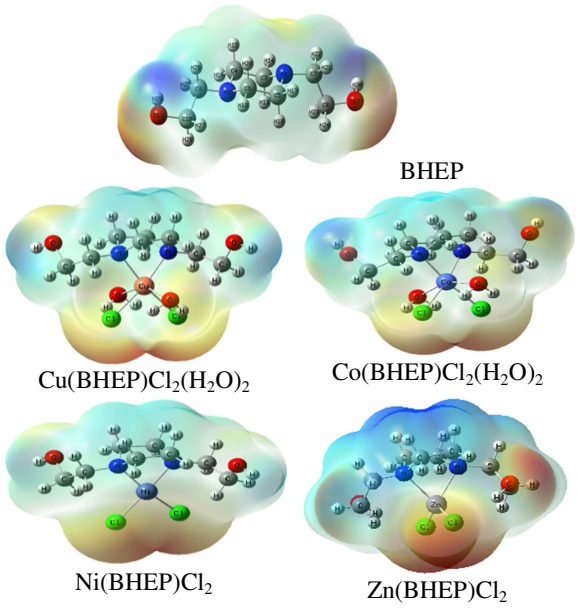

Fig. 9. Molecular electrostatic potential (MEP) surface of ligand (BHEP) and complexes (Cu(BHEP)$Cl_2(H_2O)_2$,)$_2$, Co(BHEP)$Cl_2(H_2O)_2$, Ni(BHEP)Cl_2, and Zn(BHEP)Cl_2

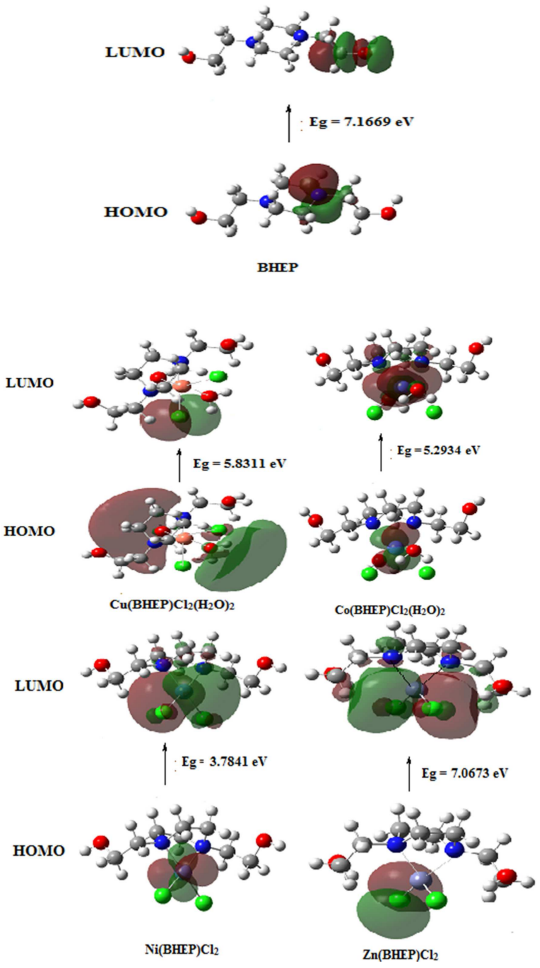

Fig. 10. HOMO and LUMO charge density maps of ligand and complexes Cu(BHEP)$Cl_2(H_2O)_2$, o(BHEP)$Cl_2(H_2O)_2$,Ni(BHEP)Cl_2 and Zn(BHEP)Cl_2

Figure 9 shows the MEP surface to locate the positive (blue color) and negative (red color, it is bound loosely or excess electrons) charged electrostatic potential in the molecule. The calculated total energy, the highest occupied molecular orbital (HOMO) and lowest unoccupied molecular orbital (LUMO) energies, and the dipole moment for the ligand and complexes were listed in Table 6. The more negative values of the total energy of the complexes than that of the free ligand indicate that the complexes are more stable than the free ligands. Also, the energy gaps (E_g) = E_{LUMO} - E_{HOMO} of complexes are smaller in the case than that of ligand due to the chelation of ligand to metalions. The polarity of the complex is much larger than the free ligand, Table 6 and Figure 10.

3.6. Antitumor activity

The in vitro antitumor activity results show that the complexes exhibit a low cytotoxic effect for breast cancer (Mcf7 cell line) as indicated by their IC_{50} values, Figure 11. The activity order isCo(II) complex (16 µg/ml) >Cu(II) complex (19 µg/ml) >Ni(II) complex (35 µg/ml) >Zn(II) complex(42 µg/ml) >BHEP (45 µg/ml).

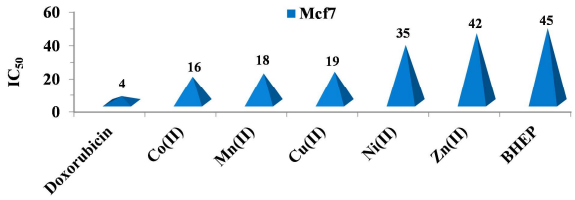

Fig. 11.IC50 Values of ligand and its complexes against breast cancer cell lines compared to Doxorubicin

3.7. Molecular docking

The structure of ligand and complexes were created in PDB file format from the output of Gaussian09 software.

The crystal structure of the receptor of breast cancer (PDB ID: 3HB5) was downloaded from the protein data bank (http://www.rcsb.org./pdb).

The molecular docking studies were performed using MOA2019 software, to find the possible binding modes of the most active sites.

3.7.1. Docking on breast cancer oxidoreductase (PDB ID: 3HB5)

In the present study, the binding free energy of ligand, and complexes with protein (PDB ID: 3HB5) receptors are found to be -8.0, -8.4, -9.7, -37.9, -38.7 and -41.9 kcal/mol for BHEP and complexes: Zn(II), Ni(II), Cu(II)and Co(II); respectively, Table 8. The more negative the binding energy the stronger interaction. So, the interactions are in the order of Co(II) complex>Cu(II) complex>Ni(II) complex >Zn(II) complex>BHEP, Table 8 and Figure 12.

The 2D and 3D plots of the interactions of ligand (BHEP), and complexes (Cu(II), Co(II), Ni(II), and Zn(II)) with the active site of the receptor of breast cancer oxidoreductase (PDB ID: 3HB5) are shown in Figure 12.

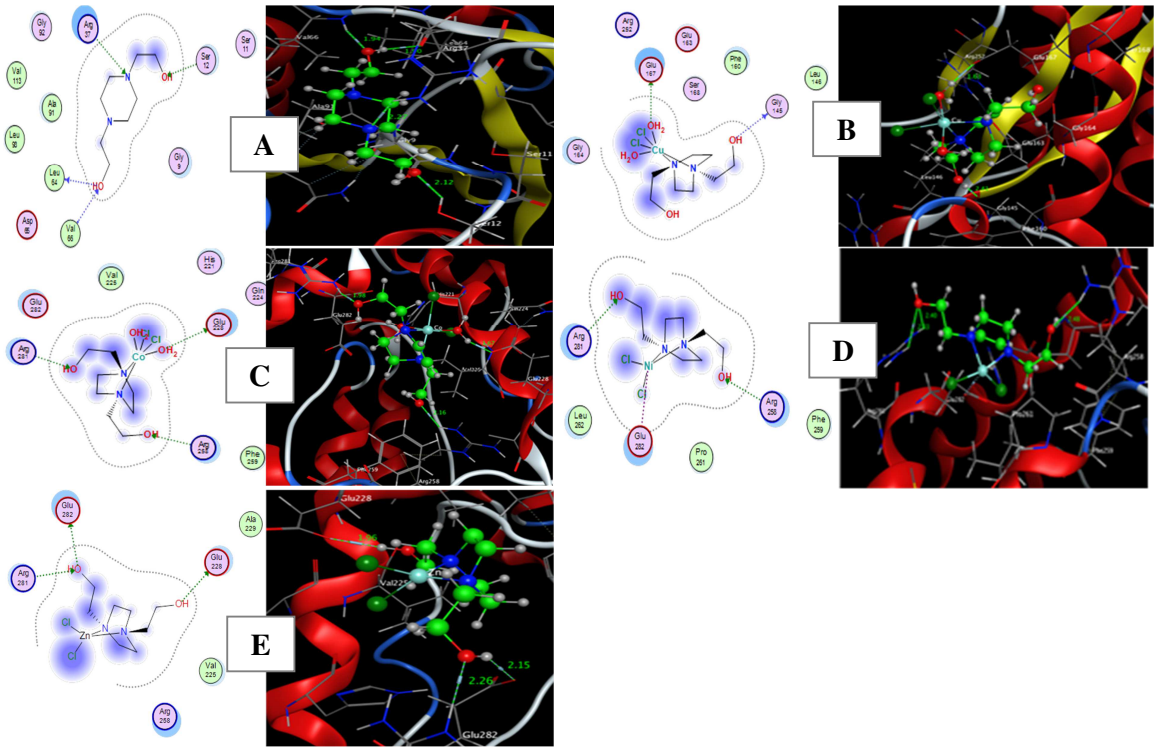

Fig. 12. Molecular docking simulation studies of the interactions between Ligand (A), Cu(II) complex (B), Co(II) complex (C), Ni(II) complex (D) and Zn(II) complex (E) with the active site of the receptor of breast cancer oxidoreductase (PDB ID: 3HB5). The docked conformation of the compound isshown in ball and stick representation.

Table 8
The Docking interaction data calculations of ligand (BHEP), and complexes (Cu(II), Co(II), Ni(II) and Zn(II)) with the active site of the receptor of breast cancer oxidoreductase (PDB ID: 3HB5)

	Receptor	Interaction	Distance(Å)*	E (Kcal/mol)
BHEP				
O 12	O LEU 64	H-donor	2.84 (1.90)	-2.0
N 2	NH2 ARG 37	H-acceptor	3.05 (2.27)	-2.9
O 11	OG SER 12	H-acceptor	2.94 (2.12)	-0.9
O 12	N VAL 66	H-acceptor	2.93 (1.94)	-2.2
Cu(II) complex				
O 11	O GLY 145	H-donor	3.35 (2.41)	-0.8
O 32	OE1 GLU 167	H-donor	2.63 (1.63)	-25.3
O 32	OE1 GLU 167	Ionic	2.63	-7.4
O 32	OE2 GLU 167	Ionic	3.01	-4.4
Co(II) complex				
O 32	OE2 GLU 228	H-donor	2.66 (1.67)	-27.2
O 11	NH1 ARG 258	H-acceptor	3.01 (2.16)	-2.0
O 12	NH2 ARG 281	H-acceptor	2.93 (1.98)	-3.4
O 32	OE1 GLU 228	Ionic	3.45	-2.1
O 32	OE2 GLU 228	Ionic	2.66	-7.2
Ni(II) complex				
O 11	NH1 ARG 258	H-acceptor	3.37 (2.48)	-1.9
O 12	NH1 ARG 281	H-acceptor	3.06 (2.33)	-2.9
O 12	NH2 ARG 281	H-acceptor	3.11 (2.40)	-2.0
NI 29	OE2 GLU 282	Metal	2.43	-2.9
Zn(II) complex				
O 11	OE2 GLU 228	H-donor	2.94 (1.96)	-3.7
O 12	OE2 GLU 282	H-donor	3.04 (2.15)	-2.8
O 12	NH1 ARG 281	H-acceptor	3.15 (2.26)	-1.9

4. Conclusions

The present study shows that the measured acid dissociation constants of the protonated BHEP are corresponding to the piperazine nitrogen atoms. The investigation of complex formation with different metal ions reveals the formation of 1:1 and 1:2 complexes. The formation constants were calculated. The log β_1 values were found in the order Co < Ni < Cu > Zn, which is following Irving-Williams order. The concentration distribution diagrams were evaluated. The thermodynamic parameters as ΔG, ΔH and ΔSforthe protonation of BHEP and its metal complexes were estimated and discussed. DFT calculations were performed to deduce the optimized structure of BHEP and its complexes. Selected bond distances and bond angles were interpreted based on the structure of the complexes. Metal complexes were synthesized andthe compositionswere deduced from elemental analysis and mass spectra. The antitumor activity wasscreened. The computational exploration by molecular docking simulation has been carried out with the receptors of breast cancer.

5. Conflicts of interest

There are no conflicts to declare.

6. References

[1] Valverde M.G., andTorroba T., Sulphur - Nitrogen Heterocycles. Molecules. 2005;10(2), 318-320. https://doi.org/10.3390/10020318

[2] Kant, R., and Maji, S., Recent advances in the synthesis of piperazine based ligands and metal complexes and their applications. Dalton Transactions, 2021, 50(3), 785-800.https://doi.org/10.1039/D0DT03569F

[3] Shaquiquzzaman M., Verma G., Marella A., Akhter M., Akhtar W., Khan M.F., Tasneem S., andAlam M.M., Piperazine scaffold: A remarkable tool in generation of diverse pharmacological agents. European journal of medicinal chemistry, 2015; 102, 487-529.https://doi.org/10.1016/j.ejmech.2015.07.026

[4] Abu Mohsen U., Synthesis and Antimicrobial Activity of Some PiperazineDithiocarbamate Derivatives. Turk. J. Pharm. Sci.2014;11(3), 347-354.https://cms.galenos.com.tr/Uploads/Article_12341/347-354.pdf

[5] Asif M., Piperazine and Pyrazine Containing Molecules and Their Diverse Pharmaceutical Activities. International J. of Advances in Scientific Research.2015;1, 5-11. https://doi.org/10.7439/ijasr.v1i1.1766

[6] Hale S.L., andKloner R.A., Ranolazine, an Inhibitor of the Late Sodium Channel Current, reduces Postischemic myocardial dysfunction in the rabbit. J. Cardiovasc. PharmacolTher. 2006;11(4), 249 – 255. https://doi.org/10.1177/1074248406294607

[7] Fragasso G., Palloshi A., Puccetti P., Silipigni C., Rossodivita A., Pala P., Calori G., Alfieri O., andMargonato A., A randomized Clinical Trial of Trimetazidine, a partial free fatty acid oxidation inhibitor, in patients with heart failure. J. Am. Coll. Cardiol. 2006;48(5), 992-998. https://doi.org/10.1016/j.jacc.2006.03.060

[8] Kinney J.L., andEvans R.L., Evaluation of amoxapine. Clin., Pharm. 1982;1(5) , 417-424.https://europepmc.org/article/med/6764165

[9] Gastpar M., Gastpar G., andGilsdorf U., Befuraline, its safety and efficacy in depressed in patients. Pharmacopsychiarty. 1985;18(6), 351-355. https://doi.org/10.1055/s-2007-1017396

[10] Rees L., Chloropromazine and allied phenothiazine derivatives. British Med. J.1960; 2(5197), 522 – 525. https://doi.org/10.1136/bmj.2.5197.522

[11] Tang L., Shukla P.K., andWang Z.J., Trifluoperazine, an orally available clinically used drug, disrupts opioid antinociceptive tolerance. Neurosci. Lett. 2006;397(1-2), 1-4. https://doi.org/10.1016/j.neulet.2005.11.050

[12] Shehata M.R.**,** Shoukry M.M., Shokry S.A., andMabrouk M.A., Thermal stability of Pd(1,4-bis(2-hydroxyethyl)piperazine)Cl_2 and its role in the catalysis of amino acid ester. J. Coord. Chem.2015;68(17-18), 3272-3281. https://doi.org/10.1080/00958972.2015.1061659

[13] Shehata M.R.**,** Shoukry M.M., Shokry S.A., Mabrouk M.A., andVan Eldik R., Synthesis, X-ray structure, DFT and thermodynamic studies of mono- and binuclear palladium(II) complexes involving 1,4-bis(2-hydroxyethyl)piperazine, bio-relevant ligands and 4,4′-bipiperidine. J. Coord. Chem.2016;69 (3), 522-540. http://dx.doi.org/10.1080/00958972.2015.1132312

[14] Shehata M.R., Shoukry M.M., Shokry S.A., Mabrouk M.A., Kozakiewicz A., andVan Eldik R., Studies on Pd(1,4-bis(2-hydroxyethyl)piperazine)dicarboxylic acid complexes as models for carboplatin with structural features enhancing the interaction with DNA. J. Coord. Chem.2019;72(12), 2035-2049. https://doi.org/10.1080/00958972.2019.1632441

[15] El-Sherif A.A., Shehata M.R.**,** Shoukry M.M., andMahmoud N., Potentiometric study of speciation and thermodynamics of complex formation equilibria of diorganotin(IV) dichloride with 1-(2-aminoethyl)piperazine. J. Sol. Chem. 2016;45, 410-430. https://doi.org/10.1007/s10953-016-0450-5.

[16] Shehata M.R., Mohamed M.M.A., Shoukry M.M., Hussein M.A., andHussein F.M., Synthesis, characterization, equilibria and biological activity of dimethyltin(IV) complex with 1,4-piperazine. J. Coord. Chem. 2015;68(6), 1101-1114. https://doi.org/10.1080/00958972.2015.1007962

[17] Shoukry M.M., Shehata M.R., andAbdel Wahab A.M., Synthesis, characterization, thermal degradation, docking, DFT calculation, and biological activity of dimethyltin(IV) complex with homopiperazine. Journal of the Chinese Chemical Society, 2021;68(11), 2164-2176. https://doi.org/10.1002/jccs.202100227

[18] Welcher F. J., The Analytical Uses of Ethylenediaminetetraacetic Acid, Princeton: Van Nostrand. 1965.

[19] BatesR.G.. Determination of pH: Theory and Practice, 2nd ed. New York: Wiley Interscience; 1977.

[20] Al-Flaijj O., Shehata M.R., Mohamed M.M.A. and Shoukry M.M.,Manatsheftefürchemie., 2001;132,349-366. https://doi.org/10.1007/s00706017012

[21] Hay R.W. and You-Quan C., Polyhedron, 14 (1995) 869-872.https://doi.org/10.1016/0277-5387(94)00324-8

[22] Gans P., Sabatini A.,and Vacca A., An improved computer program for the computation of formation constants from potentiometric data. InorgChimActa. 1976;18:237–239. https://doi.org/10.1016/S0020-1693(00)95610-X

[23] L. Pettit, Personal Communication, University of Leeds; 1993.

[24] Frisch M.J., et. al., Gaussian 09, Revision D.01 (Gaussian, Inc., Wallingford CT), 2013.

[25] C.C.G. Inc, "Molecular operating environment (MOE 2019.01)" Chemical Computing Group Inc. 1010 Sherbooke St. West, Suite # 910, Montreal, QC, Canada, H3A 2R7, (2019).

[26] Jin Z., Du X., Xu Y., Deng Y., Liu M., Zhao Y., Zhang B., Li X., Zhang L., Peng C., Duan Y., Yu J., Wang L., Yang K., Liu F., Jiang R., Yang X., You T., Liu X., Yang X., Bai F,. Liu H., Liu X., Guddat L.W., Xu W., Xiao G., Qin C., Shi Z., Jiang H., andRao Z., Yanget H., Structure of Mpro from COVID-19 Virus and Discovery of its Inhibitors. Nature.2020;582, 289–293. https://doi.org/10.1038/s41586-020-2223-y

[27] Cotton F.A., andWilkinson G., Advaned Inorganic Chemistry. London, UK: Wiley; 1962.

[28] Phillips C.S.G., andWilliams R.J.P., Inorganic Chemistry: Metals. Vol. 2. New York, NY, USA: Oxford University Press; 1966.

[29] Al Alousi, A. S., Shehata, M. R., Shoukry, M. M., Hassan, S. A., and Mahmoud, N. Coordination properties of dehydroacetic acid–binary and ternary complexes. Journal of Coordination Chemistry, 2008;61(12), 1906-1916. https://doi.org/10.1080/00958970701788859

[30] Shehata M.R., Shoukry M.M., andBarakat M.H., Coordination properties of 6-aminopenicillanic acid: Binary and ternary complexes involving biorelevant ligands. J. Coord. Chem. 2004;57(16), 1369-1386. https://doi.org/10.1080/0095897042000261935

[31] Nassar D.A., Ali O.A., Shehata M.R.andSayed A.S., Spectroscopic investigation, thermal behavior, catalytic reduction, biological and computational studies of novel four transition metal complexes based on 5-methylthiophene Schiff base type. Heliyon, 2023; 9, e16973. https://doi.org/10.1016/j.heliyon.2023.e16973